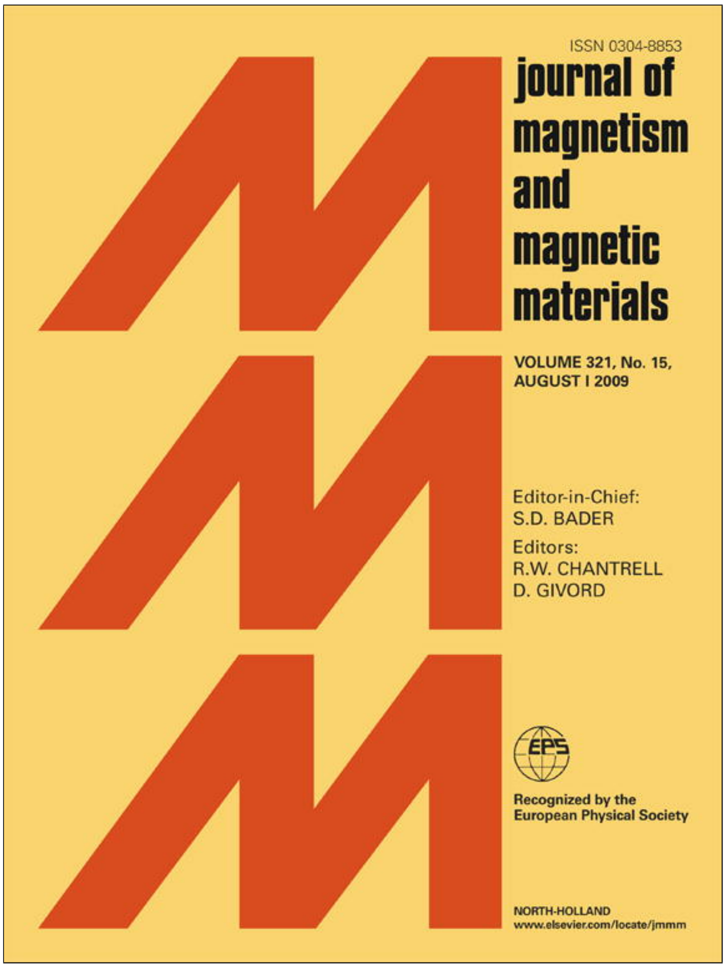
ISSN 0304-8853
journal of magnetism and magnetic materials
VOLUME 321, No. 15, AUGUST I 2009
Editor-in-Chief: S.D. BADER
Editors: R.W. CHANTRELL D. GIVORD
EPS
Recognized by the European Physical Society
NORTH-HOLLAND
www.elsevier.com/locate/jmmm

Journal of Magnetism and Magnetic Materials 321 (2009) 2304–2310

Contents lists available at ScienceDirect

Journal of Magnetism and Magnetic Materials

journal homepage: www.elsevier.com/locate/jmmm

Delocalized 2-magnons eigenstates in long-range correlated random Heisenberg chains

W.S. Dias, E.M. Nascimento, F.A.B.F. de Moura *, M.L. Lyra

Instituto de Física, Universidade Federal de Alagoas, 57072-970 Maceió, AL, Brazil

ARTICLE INFO

Article history:
Received 19 November 2008
Received in revised form
15 January 2009
Available online 27 February 2009

PACS:
73.20.Jc
75.10.Pq
75.30.Ds

Keywords:
Disordered systems
Phase transitions
Spin dynamics
Quantum localization

ABSTRACT

We consider the one-dimensional quantum disordered $S=\frac{1}{2}$ Heisenberg ferromagnetic chain model with long-range correlated exchange couplings and study the nature of collective two-spin excitations. By using an exact diagonalization of the Hamiltonian in the two-spin flip subspace, we compute the spin wave participation number to characterize the localized or delocalized nature of the two-magnon states. For strongly correlated random exchange couplings, extended two-spin excitations with finite energy appear. Integrating the time-dependent Schroedinger equation, we follow the time-evolution of an initially localized two-spin state. We find that, associated with the emergence of extended spin waves, the wave-packet mean-square displacement develops a ballistic spread. Further, the single-spin wave-packet acquires an asymmetric profile due to the kinematic interaction between the excited spins.

1. Introduction

The Anderson theory plays a key role on the localization properties of eigenfunctions in disordered systems [1,2]. The localization–delocalization transition for weak disorder in three-dimensional geometries, and its absence in low dimensional systems with time reversal symmetry at any disorder strength, are its most known predictions. The critical exponent ν that describes the divergence of the localization length $\xi_\infty \propto |E-E_c|^\nu$, where E indicates the Fermi energy and E_c stands for the mobility edges separating extended from localized states, is directly related to the exponent μ for the conductivity at zero temperature in doped semiconductors and amorphous materials [3–5]. The localization of collective excitations by a random potential is a quite general feature. It applies, for example, to the study of magnon localization in random ferromagnets and vibrational modes in harmonic systems. In fact, it is possible to map the Heisenberg Hamiltonian, as well as the one-dimensional harmonic chain with random masses, into the Anderson model for disordered electronic systems with correlated disorder [6–10,14,15].

Several works have been devoted to the study of the localization properties of spin waves in low dimensional quantum Heisenberg ferromagnets. Localization is known to have a profound impact on the transport properties of magnetic systems. In general, it has been demonstrated that the finite energy spin waves are exponentially localized for any degree of disorder. However, the typical localization length diverges as one approaches to the bottom of the band [6–9]. In addition, it was shown that an initially localized spin excitation may exhibit a super-diffusive spread in the presence of disorder in contrast to the random oscillations over a finite segment displayed by an electronic wave-packet [9,10]. Further, the diffusion of spin waves in ferromagnetic host systems with antiferromagnetic impurities shows no evidence of strong localization [11]. Also, the effects of localization in the spin and charge conductivity of ferromagnetic systems have been theoretically evaluated [12,13]. Recently, the one-dimensional quantum Heisenberg ferromagnet with exchange couplings exhibiting long-range correlated disorder was studied [14]. Using renormalization group, integration of the equations of motion and exact diagonalization, it was shown that extended states appears for sufficiently strong correlations. In fact, correlated disorder was shown to be a key ingredient to promote delocalization in low dimensional systems [16–20].

Some static and dynamic properties associated with the two-magnon excitations in finite $S=\frac{1}{2}$ ferromagnetic chains with uncorrelated disorder were studied in Ref. [21]. As a $S=\frac{1}{2}$ spin only allows for a single excitation, i.e., two-spin excitations can never occupy the same site, the effective spin–spin interaction is

* Corresponding author.
E-mail address: fidelis@if.ufal.br (F.A.B.F. de Moura).

0304-8853/$ - see front matter © 2009 Elsevier B.V. All rights reserved.
doi:10.1016/j.jmmm.2009.02.120

closely related to an infinite strength Hubbard repulsion. It was shown that the localization length of high-energy states are rather small but diverges as one approaches the ground state energy. The long localization length of the low-energy states give rises to strong spin–spin correlations which are suppressed at high energies as the localization length becomes smaller than the chain size. Further, the time-evolution of two initially localized spin deviations was followed. It was shown that the single-spin wave-packet develops asymmetric tails due to the effective spin–spin repulsion with distinct scaling exponents governing the temporal evolution of length scales related to the average spin–spin distance and the wave-packet dispersion [21].

In this work, we study the two-magnon excitations in the one-dimensional quantum disordered $S=\frac{1}{2}$ Heisenberg ferromagnet chain model with long-range correlated exchange couplings. By using an exact diagonalization approach, we compute the spin–wave participation number which will be used as a measure of the spacial extension of the two-spin excitations. The numerical calculations indicate that, in the regime of strongly correlated random exchange couplings, there are extended spin waves with finite excitation energies. We will also follow the time-evolution of the mean-square displacement of the wave-packet. We will explore the influence of the kinematic repulsion between the two magnons and the emergence of extended states on the dynamics of two-spin excitations.

2. Model and formalism

We will consider finite disordered chains with N spins ($S=\frac{1}{2}$) coupled via a first neighbors isotropic Heisenberg exchange interaction, whose Hamiltonian can be written as

$$H=-\sum_n J_{n,n+1}\vec{S_n}.\vec{S}_{n+1}. \quad (1)$$

The couplings $J_{n,n+1}=J_n$ will be considered as long-range correlated random ferromagnetic exchange integrals. In order to generate exchange sequences with power-law decaying pair correlation function, we firstly generate the following auxiliary sequence:

$$x_n=\tanh\left[\sum_{k=1}^{N/2}\frac{1}{k^{\alpha/2}}\cos\left(\frac{2\pi nk}{N}+\phi_k\right)\right], \quad (2)$$

which is restricted to the interval $-1\leqslant x_n\leqslant 1$ and whose pair correlation function decays asymptotically as $1/r^{\alpha}$. The hyperbolic transformation of the series brings the advantage of bounding the interval of the random variable without changing its asymptotic correlation function. Such power-law decaying correlation function actually characterizes the absence of a typical correlation length in the disorder distribution and allows the investigation of the influence of scale-free disorder on the properties of the collective magnetic excitations. In the above equation, k is the wave-vector of the modulations on the random variable landscape, ϕ_k are $N/2$ random phases uniformly distributed in the interval $[0,2\pi]$ and the exponent α controls the degree of correlations. The sequence of exchange integrals is obtained after normalizing the auxiliary sequence to have unitary variance (Δx) and displacing it to avoid negative (antiferromagnetic) couplings. In the following, we use $J_n=2+x_n/\Delta x$. With the above procedure, the distribution of couplings has sharp edges for any value of α, which results on long-range correlated sequences of strictly ferromagnetic couplings even when very large chains are considered.

For $\alpha=0$, we recover an uncorrelated random ferromagnetic couplings distribution. The ground state for a ferromagnetic chain consists of a perfectly ordered chain with all spins aligned on the same direction. We will refer to the ground state as the vacuum state $|0\rangle$ in what concerns to the presence of magnetic excitations. One-magnon states are the Hamiltonian eigenstates on the sub-space generated by all single flip states $|\phi_n\rangle=S_n^-|0\rangle$. In the presence of disorder, the one-magnon states are spatially localized, with the characteristic localization length diverging as one approaches the bottom of the excitation energy band. Here, we will explore the nature of the Hamiltonian eigenstates on the sub-space generated by all two flip states. The basis for this sub-space can be represented by $|\Phi_{n_1,n_2}\rangle=S_{n_1}^-S_{n_2}^-|0\rangle$ where $|\phi_{n_1,n_2}\rangle$ is the state with spin flips located at sites n_1 and n_2.

In order to characterize the nature of the two-magnon eigenstates, we solve the time-independent Schroedinger equation to obtain the coefficients ϕ_{n_1,n_2} in the expansion over the two-flip bases $|\Phi\rangle=\sum\phi_{n_1,n_2}|\phi_{n_1,n_2}\rangle$. The coefficients obey the following recursion relation:

$$\begin{aligned}2\varepsilon\phi_{n_1,n_2}&=(J_{n_1-1,n_1}+J_{n_1,n_1+1}+J_{n_2-1,n_2}+J_{n_2,n_2+1})\phi_{n_1,n_2}\\&-J_{n_1,n_1+1}\phi_{n_1+1,n_2}-J_{n_2,n_2+1}\phi_{n_1,n_2+1}\\&-J_{n_1,n_1-1}\phi_{n_1-1,n_2}-J_{n_2-1,n_2}\phi_{n_1,n_2-1}\end{aligned} \quad (3)$$

for the case of n_1 and n_2 not being neighboring sites. The eigenstate coefficient for spin flips at neighboring sites follows a simpler recursive relation in the form:

$$\begin{aligned}2\varepsilon\phi_{n,n+1}&=(J_{n-1,n}+J_{n+1,n+2})\phi_{n,n+1}-J_{n+1,n+2}\phi_{n,n+2}\\&-J_{n-1,n}\phi_{n-1,n+1}.\end{aligned} \quad (4)$$

The above set of $N(N-1)/2$ equations provides the coefficients of all two-magnon eigenstates. As the numerical algorithm requires the diagonalization of $M\times M$ matrices, with $M=N(N-1)/2$, we are restricted to compute the two-magnon states on relatively small chains. In order to infer about the limit of infinite chains, we will employ a finite-size scaling analysis. In the next section, we will show results derived from the stationary states on chains with $N=21$, 41, 81 and 101 spins. Distinct realizations of the distribution of exchange couplings will be used to perform a configurational average over the disorder, namely 8000 realizations for the smallest chain size and 500 realizations for the largest one. In order to study the spacial distribution of the two-magnon states, we computed the participation number of each eigen-state defined as

$$P=\frac{1}{\sum_{n_1<n_2}|\phi_{n_1,n_2}|^4}. \quad (5)$$

For extended two-magnon states, the participation number shall scale as N^2 (actually the maximum participation number is $M=N(N-1)/2$ for a uniform state). The states with localization lengths much smaller than the chain size have size-independent participation numbers. In addition, we will investigate the time evolution of a wave-packet initially composed of two flipped spins at a distance d_0. We solve numerically the time-dependent Schroedinger equation $i\hbar d/dt|\Phi(t)>=H|\Phi(t)\rangle$ where H is Hamiltonian (1) and $|\Phi(t)\rangle=\sum_{n_1<n_2}\phi_{n_1,n_2}(t)|\phi_{n_1,n_2}\rangle$. The time-dependent coefficients $\phi_{n_1,n_2}(t)$ obey a set of differential equations, derived from (4), for spin deviations at neighboring sites and from (3) for non-neighboring deviations, namely

$$\begin{aligned}i\frac{d\phi_{n,n+1}(t)}{dt}&=(J_{n-1,n}+J_{n+1,n+2})\phi_{n,n+1}(t)-J_{n+1,n+2}\phi_{n,n+2}(t)\\&-J_{n-1,n}\phi_{n-1,n+1}(t)\end{aligned} \quad (6)$$

and

$$i\frac{d\phi_{n_1,n_2}(t)}{dt} = (J_{n_1-1,n_1} + J_{n_1,n_1+1} + J_{n_2-1,n_2} + J_{n_2,n_2+1})\phi_{n_1,n_2}(t) - J_{n_1,n_1+1}\phi_{n_1+1,n_2}(t) - J_{n_2,n_2+1}\phi_{n_1,n_2+1}(t) - J_{n_1,n_1-1}\phi_{n_1-1,n_2}(t) - J_{n_2-1,n_2}\phi_{n_1,n_2-1}(t),$$

$$n_2 > n_1 + 1, \quad (7)$$

where we used units of $\hbar = 1$. We solved these equations numerically by using a high-order method based on the Taylor expansion of the evolution operator:

$$V(\Delta t) = \exp(-iH\Delta t) = 1 + \sum_{l=1}^{n_o} \frac{(-iH\Delta t)^l}{l!}, \quad (8)$$

where H is the Hamiltonian. The wave-function at time Δt is given by $|\Phi(\Delta t)\rangle = V(\Delta t)|\Phi(t=0)\rangle$. The method can be used recursively to obtain the wave-function at time t. The following results were taken by using $\Delta t = 0.05$ and the sum was truncated at $n_o = 20$. This cutoff was sufficient to keep the wave-function norm conservation along the entire time interval considered. We followed the time-evolution of the spacial extension of the two-magnon states defined as

$$\xi(t) = \sum_{n_1<n_2} |\phi_{n_1,n_2}(t)|^2 \sqrt{(n_1 - \langle n_1(t)\rangle)^2 + (n_2 - \langle n_2(t)\rangle)^2}, \quad (9)$$

where

$$\langle n_i(t)\rangle = \sum_{n_1<n_2} n_i |\phi_{n_1,n_2}(t)|^2, \quad i = 1, 2. \quad (10)$$

The spacial extension $\xi(t)$ gives a measure of the wave-function spread on the $n_1 \times n_2$ plane.

3. Results

In Fig. 1, we show results for the scaled participation number $P(E)/M$ ($M = N(N-1)/2$) versus energy E taking into account all states within a small energy window around E. Results were obtained using exact diagonalization on chains with $N = 41$, 61, 81 and 101 sites and (a) $\alpha = 0$ and (b) $\alpha = 3$. For $\alpha = 0$ our results show that the high-energy states are well localized presenting a short localization length. The collapse of data from distinct chain sizes at $E = 0$ indicates that the low-energy spin excitations have finite localization lengths much larger than the chain sizes considered. The normalized participation has a pronounced decrease around $E \simeq 6$. This is the typical energy scale that delimits the pseudo-band edge above which the density of states decays exponentially and the states are strongly localized. For $\alpha = 3$ the scaled participation number $P(E)/M$ displays a well-defined data collapse in the low energy regime. This result suggests the existence of a phase of extended two-magnons states. We collected in Fig. 2 results for the scaled participation function near the band bottom $P(E<1)/M$ versus the exponent α of the power-law spectral density of the correlated potential for lattices with $N = 41$, 61, 81, 101 sites. For $\alpha > 2$ the scaled participation function $P(E<1)/M$ becomes size independent, i.e., the participation function is proportional to $M = N(N-1)/2$. This feature is a clear signature of the existence of extended sates at the band bottom for $\alpha > 2$.

The time evolution of the spacial extension $\xi(t)$, obtained by numerical integration of the time-dependent Schroedinger equation, is shown in Fig. 3. A configurational average over 30 distinct runs was employed in chains with $N = 2000$ sites. In the absence of correlations ($\alpha = 0$), a diffusive-like spread, $\xi(t) \propto t^{0.50(5)}$, is observed after a short transient. This behavior is in agreement with the previous literature on the dynamics of one and two-magnons in uncorrelated random ferromagnets [9,21]. For $\alpha = 3$, the wave-packet presents a ballistic spread before reaching the lattice boundaries $\xi(t) \propto t^1$. This result gives further support to the previous indication that this ferromagnetic chain displays a

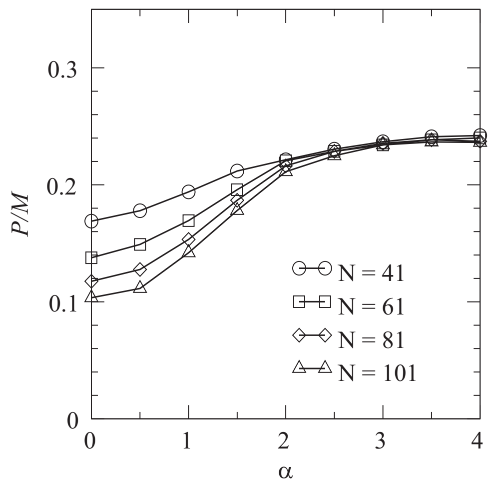

Fig. 2. Scaled participation number P/M ($M = N(N-1)/2$) versus α for $N = 41$, 61, 81 and 101. For $\alpha > 2$, P/M is roughly size independent indicating extended states.

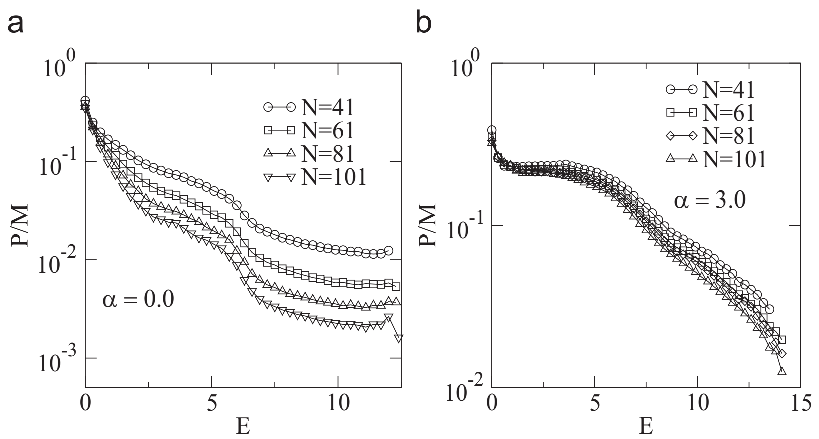

Fig. 1. Scaled participation number P/M ($M = N(N-1)/2$) versus energy for (a) $\alpha = 0$ and (b) $\alpha = 3$. The data collapse observed in the low-energy regime of the strongly correlated chain is a signature of extended two-magnon states.

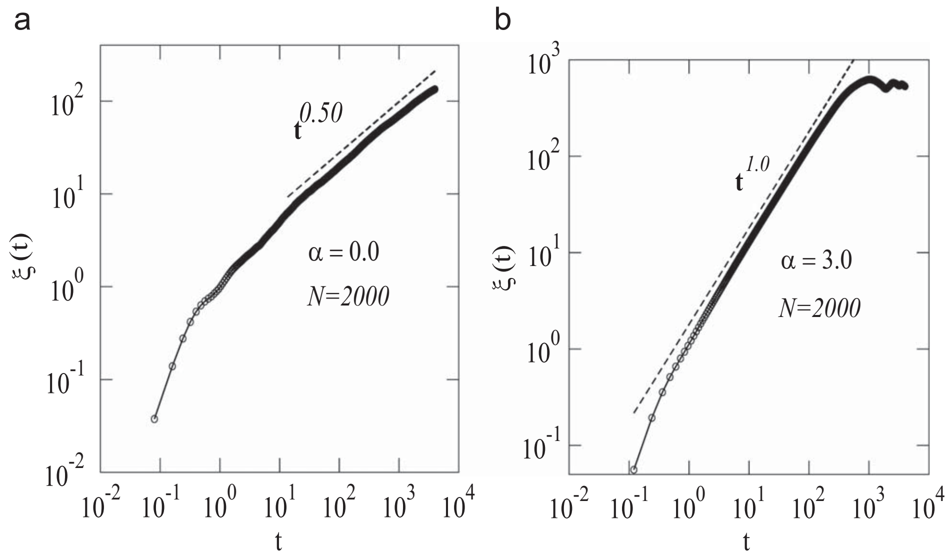

Fig. 3. The spacial extension $\xi(t)$ versus time t for $N = 2000$ and for (a) $\alpha = 0$ and (b) $\alpha = 3$. For $\alpha = 0$, the spacial extension $\xi(t)$ displays an asymptotic diffusive spread, $\xi(t) \propto t^{0.5}$. For $\alpha = 3$, the spacial extension shows a ballistic dynamics $\xi(t) \propto t^1$.

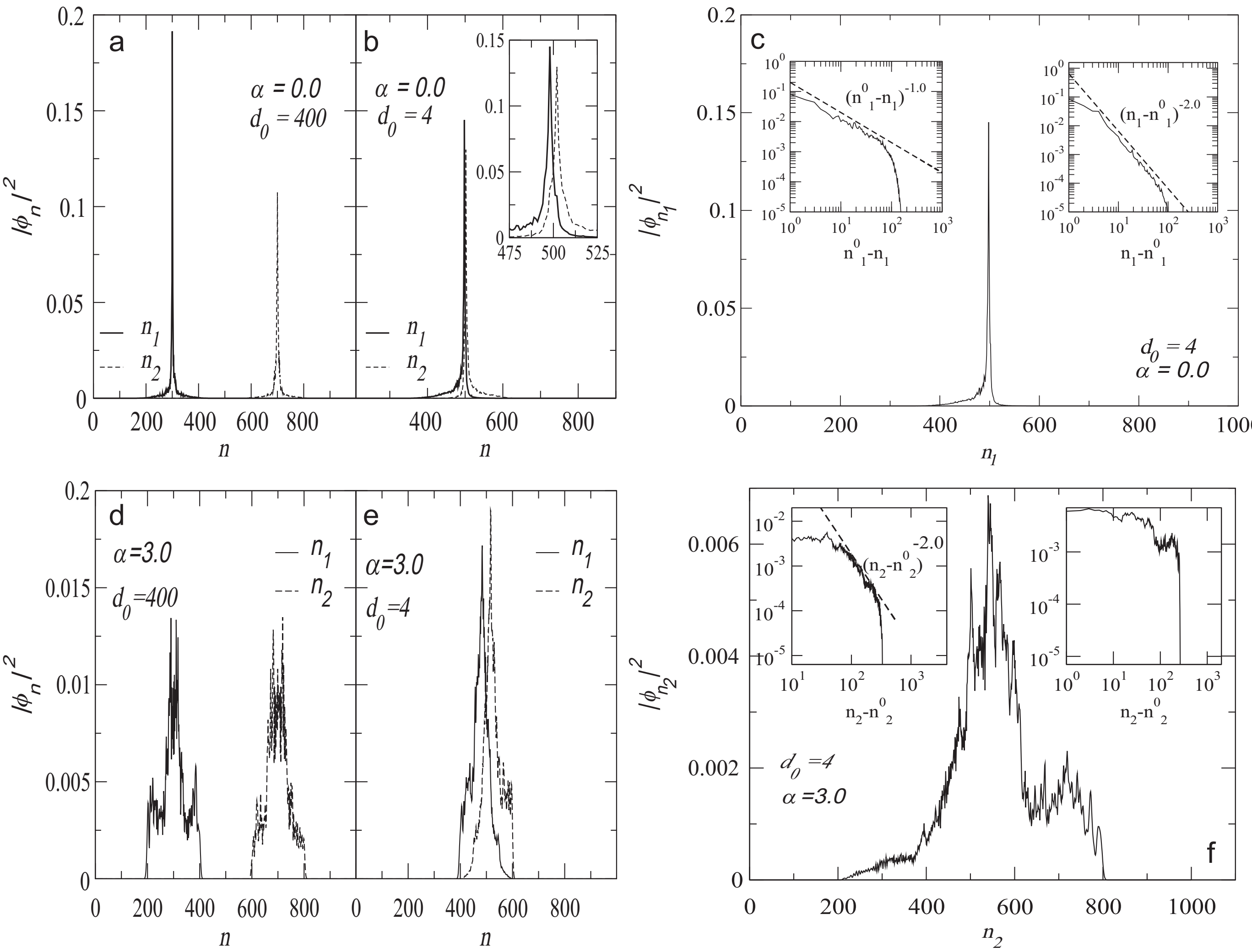

Fig. 4. (a–c) Asymptotic distribution of the single-spin wave-packet in a chain with $N = 1000$ spins with random uncorrelated exchange couplings ($\alpha = 0$). Calculations were averaged over 50 realizations. The initial state have spin deviations at sites $n_1 = N/2 - d_0$ and $n_2 = N/2 + d_0$. Notices that the wave-packet exhibits asymmetric tails for small d_0. The insets (b and c) characterize the power-law decay of each tail. The larger decay exponent of the right side of the wave-packet reflects the effective repulsion between the spin deviations. The cutoff is a finite-time effect. Asymmetric profiles were also obtained in the regime of strongly correlated disorder (d–f) for $\alpha = 3$. In the internal region the same quadratic decay obtained for the uncorrelated case is achieved. In the exterior region, only the finite-time cutoff is present with no power-law regime.

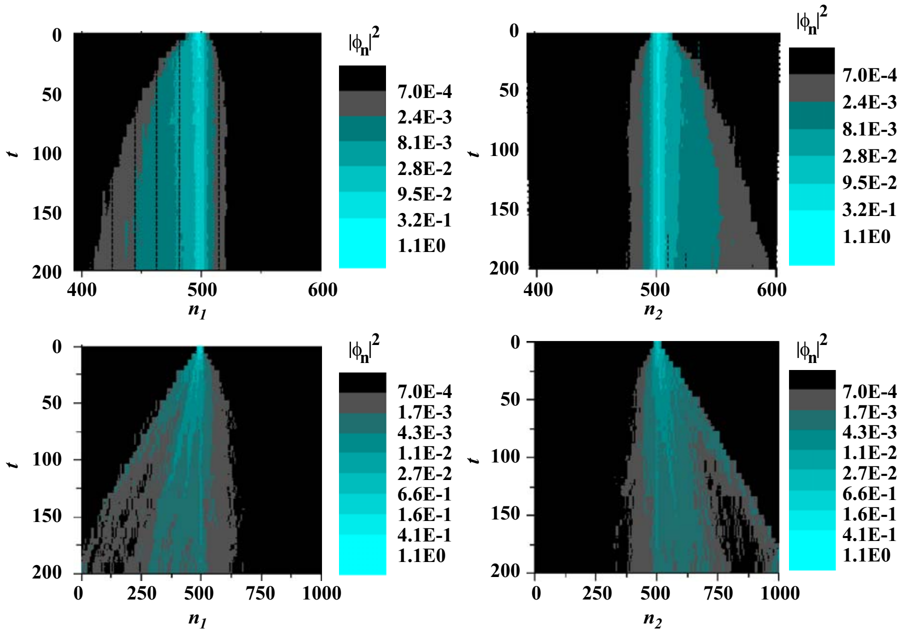

Fig. 5. Time evolution of the wave-function $|\phi_n(t)|^2$ versus t and n computed using $N = 1000$, $d_0 = 2$ and $\alpha = 0$ (a) and $\alpha = 3$ (b). For $\alpha = 0$ a finite fraction of the wave-packet remains trapped on the initial site. For $\alpha = 3$ the wave-packet spread is ballistic towards the free chain side. In both cases, the wave-packet spreads slower towards the region where the second spin flip is located due to the effective kinematic repulsion between the spins.

phase of extended two-magnons states induced by long-range correlated exchange couplings.

The long-time one-magnon wave-packet is strongly influenced by the effective kinematic interaction between the two magnons. In Fig. 4, we report the one-magnon wave-packet profile ($|\phi_n|^2 = \sum_m |\phi_{n,m}(t)|^2$) computed using $N = 1000$, $\alpha = 0$ and $d_0 = 200$ (a) and $d_0 = 4$ (b,c). One notices in (b) and (c) that the single-spin wave-packet develops power-law tails with distinct characteristic exponents on each side. The larger decay exponent is a consequence of the effective repulsion between the spins which difficult the single-spin wave-packet to spread towards the region predominantly occupied by the second spin excitation. For $d_0 = 200$, no distortion of the single-spin wave-packet was observed, reflecting the absence of effective interaction between the spins up to the time scale reported (see Fig. 4(a)). In the presence of strongly correlated disorder (see Fig. 4(d–f)) the distortion of the single-spin wave-packet was also detected for small d_0. In this case, due to the presence of an energy band of extended states, the width of each spin wave-packet becomes much larger than in (a–c) case for $\alpha = 0$. Therefore, the effective repulsion between the spins is stronger resulting in a highly asymmetric profile. The same quadratic decay results from the kinematic repulsion. In the exterior region, no power-law regime sets up. The wave-packet just exhibits a sharp cutoff that signals the wave-packet front. The structure observed in these wider wave-packets reflects the random nature of the underlying exchange integrals which promotes random scattering of the wave-packet. The asymmetric time-evolution of the wave-packet is more clearly illustrated in Fig. 5 which shows the time-evolution of both magnons through the lattice. This calculation was done using $N = 1000$, $d_0 = 4$ and $\alpha = 0$ (a) and $\alpha = 3$ (b). The effective kinematic repulsion between the spins is reflected by the small spread of the wave-packet toward the region occupied by the second spin excitation, an effect which is quite more evident in the case of strongly correlated exchanges.

Finally, we study in Fig. 6 the time dependence of the wave-packet centroid of both magnons ($\langle n_1(t)\rangle$ and $\langle n_2(t)\rangle$), as well as the time dependence of the correlation function $\zeta(t) = \langle n_1(t)n_2(t)\rangle - \langle n_1(t)\rangle\langle n_2(t)\rangle$. These calculations were performed for $N = 2000$, and two typical values of d_0 and α. In agreement with Figs. 5 and 6, these figures further characterize the role played by the effective kinematic repulsion between the spins. Particularly, a pronounced collision effect is observed for $\alpha = 3$ (see Fig. 6(d)). It results from the competition between the ballistic propagation driven by the extended states and the effective kinematic repulsion. In Fig. 6(e), the time dependent correlation function for $\alpha = 0$ is only weakly increasing with time reflecting the localized character and the diffusive spread of both magnons. On the other hand, $\zeta(t)$ grows much faster for $\alpha = 3$ corroborating our previous finding of a strong repulsion due to the presence of extended two-magnon states in the regime of long-range correlated disorder. The initial plateaus represent the regime on which the two excitations have a negligible overlap. In this regime, the correlation function is very small and below the accuracy of the numerical integration of the time-dependent Schroedinger equation. The discontinuity of the derivative actually signals the collision time after which the magnons start to repel each other.

4. Summary and conclusions

In summary, we investigated some stationary and dynamical aspects of two-magnon excitations in one-dimensional quantum disordered $S = \frac{1}{2}$ Heisenberg ferromagnet chains with long-range correlated exchange couplings. To introduce long-range correlations in this system, we considered a Fourier method to construct a on-site energy sequence with spectral density $S(k) \propto 1/k^{\alpha}$. Using an exact diagonalization formalism, we investigated the participation function of all energy eigenstates. For weakly correlated exchange couplings ($\alpha < 2$), the two-magnons states remain exponentially localized, similar to the Anderson localization of single-spin collective excitations. The high-energy spin-excitations have rather small localization lengths. However, the

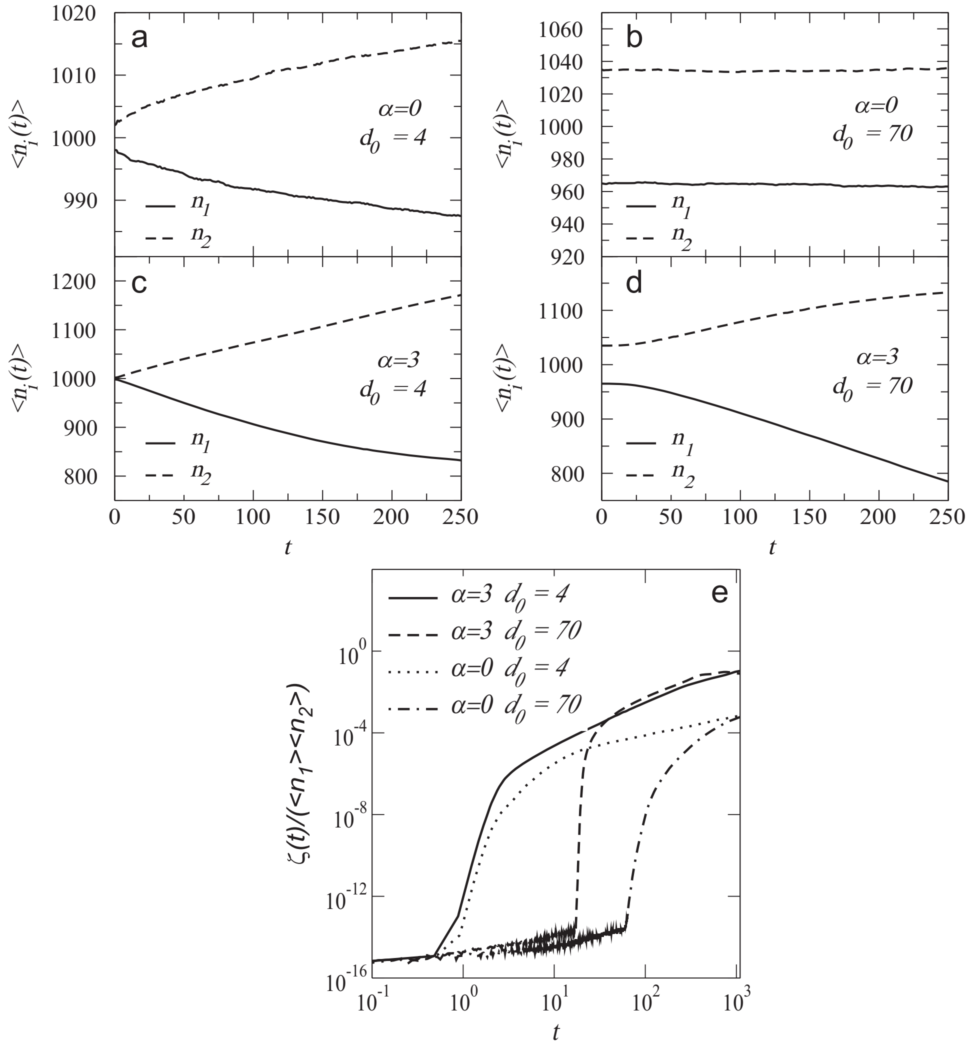

Fig. 6. (a–d) Time dependent wave-packet centroid of both magnons ($\langle n_1(t)\rangle$ and $\langle n_2(t)\rangle$) as well as (e) the time dependent correlation function $\zeta(t) = \langle n_1(t)n_2(t)\rangle - \langle n_1(t)\rangle\langle n_2(t)\rangle$. Calculations were done for $N = 2000$, $d_0 = 4$ and 70, while $\alpha = 0$ and 3. Notice that the kinematic interaction repels the wave-packet centroids. This effect is enhanced in the regime of strongly correlated disorder which results in more correlated wave-packets. The initial plateaus in the time-dependent correlation function is due to the finite accuracy of the numerical integration and actually represent the regime on which the two excitations have a negligible overlap.

localization length diverges as one approaches to the ground state. The numerical calculations indicated that, for strongly correlated random exchange couplings, extended spin waves appear for nonzero energies. Using the participation number scaling near the band bottom, we showed that a band of extended states appears for $\alpha > 2$. By integration of the time-dependent Schroedinger equation, we computed the mean-square displacement of the wave-packet. We found that, associated with the emergence of extended spin waves for $\alpha > 2$, the wave-packet mean-square displacement displays a ballistic spread, in contrast with the diffusive dynamics in the case of uncorrelated random exchanges. This result further characterizes the extended nature of the low-energy states in the strongly correlated regime. Moreover, we showed that the one-magnon wave-packet develops an asymmetric profile due to the effective kinematic repulsion between the magnons. In the interior region of the chain, the wave-packet develops a quadratically decaying tail irrespective to the presence of correlations. On the other hand, the $1/r$ decay typical of uncorrelated random ferromagnets, associated with the diffusive spread to the exterior region, is replaced by a sharp cutoff in the presence of strong correlations with no intermediate power-law regime. The combined effect of the kinematic repulsion and ballistic dynamics in the strongly correlated regime leads to the build up of spin–spin correlations which are substantially larger than in ferromagnetic chains with uncorrelated disorder. We hope that the present work will stimulate further studies of the transport of interacting magnetic excitations in correlated disordered magnets.

Acknowledgments

This work was partially supported by CNPq-Rede Nanobioestruturas, CAPES (Brazilian research agencies) and FAPEAL (Alagoas State agency).

References

[1] T.A.L. Ziman, Phys. Rev. Lett. 49 (1982) 337
For a review see, e.g., B. Kramer, A. MacKinnon, Rep. Prog. Phys. 56 (1993) 1469.

[2] E. Abrahams, P.W. Anderson, D.C. Licciardello, T.V. Ramakrishnan, Phys. Rev. Lett. 42 (1979) 673
For a review see, e.g., I.M. Lifshitz, S.A. Gredeskul, L.A. Pastur, Introduction to the Theory of Disordered Systems, Wiley, New York, 1988.
[3] K. Slevin, T. Ohtsuki, Phys. Rev. Lett. 82 (1999) 382.
[4] K. Slevin, T. Ohtsuki, Phys. Rev. Lett. 78 (1997) 4083.
[5] Y. Asada, K. Slevin, T. Ohtsuki, J. Phys. Soc. Jpn. Suppl. 74 (2005) 238.
[6] T.A.L. Ziman, Phys. Rev. Lett. 49 (1982) 337.
[7] G. Theodorou, J. Phys. C 15 (1982) L1315.
[8] R. Riklund, M. Severin, J. Phys. C 21 (1988) L965.
[9] S.N. Evangelou, D.E. Katsanos, Phys. Lett. A 164 (1992) 456.
[10] S.N. Evangelou, A.Z. Wang, S.J. Xiong, J. Phys. Condens. Matter 6 (1994) 4937.
[11] M. Crisan, L. Tataru, J. Magn. Magn. Mater. 138 (1994) 57.
[12] V.K. Dugaev, P. Bruno, J. Barnaś, J. Magn. Magn. Mater. 240 (2002) 200.
[13] V.K. Dugaev, P. Bruno, J. Barnaś, J. Magn. Magn. Mater. 242 (2002) 461.
[14] F.A.B.F. de Moura, M.D. Coutinho-Filho, E.P. Raposo, M.L. Lyra, Phys. Rev. B 66 (2002) 014418.
[15] P. Dean, Proc. Phys. Soc. 84 (1964) 727.
[16] F.M. Izrailev, A.A. Krokhin, Phys. Rev. Lett. 82 (1999) 4062;
F.M. Izrailev, A.A. Krokhin, S.E. Ulloa, Phys. Rev. B 63 (2001) 41102.
[17] F.A.B.F. de Moura, M.L. Lyra, Phys. Rev. Lett. 81 (1998) 3735;
F.A.B.F. de Moura, M.L. Lyra, Physica A 266 (1999) 465.
[18] F.A.B.F. de Moura, M.D. Coutinho-Filho, E.P. Raposo, M.L. Lyra, Phys. Rev. 68 (2003) 012202.
[19] F. Domínguez-Adame, V.A. Malyshev, F.A.B.F. de Moura, M.L. Lyra, Phys. Rev. Lett. 91 (2003) 197402.
[20] F.A.B.F. de Moura, M.D. Coutinho-Filho, E.P. Raposo, M.L. Lyra, Europhys. Lett. 66 (2004) 585.
[21] E.M. Nascimento, F.A.B.F. de Moura, M.L. Lyra, Phys. Rev. B 72 (2005) 224420.